

# Lumped-elements tunable frequency selective surfaces

**Citation for published version (APA):**

Keyrouz, S., Perotto, G., & Visser, H. J. (2014). Lumped-elements tunable frequency selective surfaces. In *Proceedings of the 8th European Conference on Antennas and Propagation (EuCAP 2014), 6-11 April 2014, The Hague, The Netherlands* (pp. 475-478). Institute of Electrical and Electronics Engineers.  
<https://doi.org/10.1109/EuCAP.2014.6901795>

**DOI:**

[10.1109/EuCAP.2014.6901795](https://doi.org/10.1109/EuCAP.2014.6901795)

**Document status and date:**

Published: 01/01/2014

**Document Version:**

Publisher's PDF, also known as Version of Record (includes final page, issue and volume numbers)

**Please check the document version of this publication:**

- A submitted manuscript is the version of the article upon submission and before peer-review. There can be important differences between the submitted version and the official published version of record. People interested in the research are advised to contact the author for the final version of the publication, or visit the DOI to the publisher's website.
- The final author version and the galley proof are versions of the publication after peer review.
- The final published version features the final layout of the paper including the volume, issue and page numbers.

[Link to publication](#)

**General rights**

Copyright and moral rights for the publications made accessible in the public portal are retained by the authors and/or other copyright owners and it is a condition of accessing publications that users recognise and abide by the legal requirements associated with these rights.

- Users may download and print one copy of any publication from the public portal for the purpose of private study or research.
- You may not further distribute the material or use it for any profit-making activity or commercial gain
- You may freely distribute the URL identifying the publication in the public portal.

If the publication is distributed under the terms of Article 25fa of the Dutch Copyright Act, indicated by the "Taverne" license above, please follow below link for the End User Agreement:

[www.tue.nl/taverne](http://www.tue.nl/taverne)

**Take down policy**

If you believe that this document breaches copyright please contact us at:

[openaccess@tue.nl](mailto:openaccess@tue.nl)

providing details and we will investigate your claim.

# Lumped-Elements Tunable Frequency Selective Surfaces

S. Keyrouz<sup>1,2</sup>, G. Perotto<sup>1</sup> and H. J. Visser<sup>2,1</sup>

<sup>1</sup>Eindhoven University of Technology, Den Dolech 2, 5612 AZ, Eindhoven, Netherlands

<sup>2</sup>Holst Centre/imec-nl, High Tech Campus 31, 5656 AE, Eindhoven, Netherlands

s.keyrouz@tue.nl

**Abstract**—This paper presents an equivalent circuit model to predict the transmission and the reflection characteristics of different Frequency Selective Surfaces (FSS). The effect of the substrate thickness and permittivity are discussed. A Gridded-Square-Loop (GSL) loaded with lumped-elements is employed to tune the reflection and the transmission characteristics of the FSS. The design method is validated for different polarizations and for different incident angles. In order to tune the response of the FSS, lumped elements (R,L,C) can be inserted in the metallic conductive grid of the FSS. The waveguide simulator method and full-wave simulations are employed to validate the derived analytical equations.

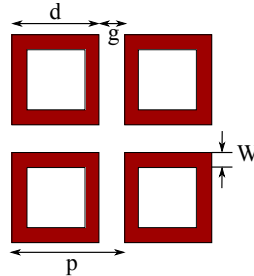
**Index Terms**—Analytical solution, frequency selective surfaces, lumped elements, waveguide simulator method.

## I. INTRODUCTION

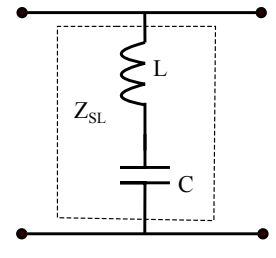
Frequency Selective Surfaces (FSSs) consist of metallic grids or patches backed on a dielectric substrate. They are employed in diverse application fields, ranging from commercial to military sectors to provide band-pass or band-stop characteristics. In the framework of antenna systems, FSSs provide frequency windows in radomes or multiband frequency operations [1]. FSSs can be used for protection from harmful electromagnetic radiation especially in domestic environment, schools and offices.

Different techniques have been adopted for the analysis of frequency selective surfaces. Including the modal analysis [2] the Iterative Process [3] and the Equivalent Circuit Model [4]. The equivalent circuit model gives a fast and considerably accurate response in describing FSS transmission and reflection characteristics, however, is only valid for certain structures and it presents some limitations (i.e. no cross-polarization response can be estimated). A simple set of equations are employed to analyze the structures. They represent the particular geometry with resonant circuits consisting of inductances and capacitances.

In this paper, the equivalent circuit model will be used to calculate the band-pass and the band-stop characteristics of different FSS structures including the square-loop FSS and the gridded-square-loop FSS. The equivalent circuit model is then extended to allow the insertion of lumped elements in the grid. The following section introduces the equivalent circuit model to characterise square-loop FSS.



(a) Square-loop FSS



(b) Equivalent circuit model

Fig. 1. Square-loop (SL) frequency selective surface and its equivalent circuit model.

## II. SQUARE-LOOP FSS

The square-loop FSS has been investigated in literature by several authors [5]–[7]. Fig. 1-a shows the unit cell of a square-loop FSS, where  $g$  is the gap between neighboring elements,  $W$  is the width of the loops  $d$  is the length of the square side and  $p = (d + g)$  is the periodicity of the unit cell. The equivalent circuit of the square-loop is shown in Fig. 1-b and is a series  $LC$  circuit where  $L$  represents the inductance due to the vertical metal conductor and  $C$  is the capacitance between the horizontal conductors.

The surface impedance of the square loop is given by:

$$Z_{fss} = j \left( X_L - \frac{1}{B_C} \right) \quad (1)$$

where  $X_L$  and  $B_C$  are derived as presented in [6]:

$$X_L = Z_0 \left( \frac{d}{p} \right) F(p, 2w, \lambda) \quad (2)$$

$$B_C = \frac{4}{Z_0} \left( \frac{d}{p} \right) F(p, g, \lambda) \quad (3)$$

where  $F_{TE,TM}(p, 2w, \lambda)$ ,  $F_{TE,TM}(p, g, \lambda)$  are derived in [8], [9],

$$F_{TE}(p, w, \lambda) = \Upsilon \left[ \ln \csc \left( \frac{\pi w}{2p} \right) + G(p, w, \lambda, \theta) \right], \quad (4)$$

$$F_{TM}(p, w, \lambda) = \Phi \left[ \ln \csc \left( \frac{\pi w}{2p} \right) + G(p, w, \lambda, \varphi) \right], \quad (5)$$

$$F_{TE}(p, g, \lambda) = \Psi \left[ \ln \csc \left( \frac{\pi g}{2p} \right) + G(p, g, \lambda, \theta) \right], \quad (6)$$

$$F_{TM}(p, g, \lambda) = \Omega \left[ \ln \csc \left( \frac{\pi g}{2p} \right) + G(p, g, \lambda, \varphi) \right], \quad (7)$$

where  $\Upsilon = \frac{p * \cos \theta}{\lambda}$ ,  $\Phi = \frac{p * \sec \varphi}{\lambda}$ ,  $\Psi = \frac{p * \sec \theta}{\lambda}$  and  $\Omega = \frac{p * \cos \varphi}{\lambda}$ .

With  $\theta$  and  $\varphi$  being the angles of incidence of a TE and a TM polarized wave respectively. The absolute value in dB of the transmission and the reflection coefficients is derived from the normalized surface impedance of the unit cell:

$$|T|_{dB} = 20 \log_{10} \left[ \frac{2Z_{fss}}{1 + 2Z_{fss}} \right], \quad (8)$$

$$|R|_{dB} = 20 \log_{10} \left[ \frac{-1}{1 + 2Z_{fss}} \right]. \quad (9)$$

TABLE I  
ANALYZED SQUARE LOOP ARRAY CONFIGURATIONS

SL Array #	p mm	d mm	g mm	w mm	t mm	$\epsilon_r$
1	10.0	8.75	1.25	0.625	0.0	1.0
2	(d+g)	21.0	-*	3.0	0.0	1.0
3	22.0	21.0	1.0	3.0	-*	2.2
4	32.25	31.0	1.25	3.0	0.25	-*

\*Parameter has been varied

In order to verify the accuracy of the analytical equations, the reflection and the transmission coefficients are calculated and compared to the results obtained by Finite Integration Technique (FIT) [10]. Table I summarizes different array configurations (in terms of dimensions and dielectric characteristics) that are investigated here. For Array #1 of Table I, the substrate effect is not included. Fig. 2 shows the magnitude and the phase of the transmission and the reflection coefficients as a function of frequency calculated by the Analytical Equations (AE) and by the finite integration technique using CST microwave Studio®.

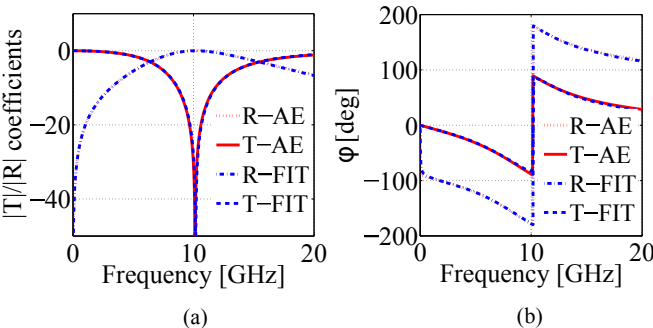


Fig. 2. Magnitude (a) and phase (b) of reflection and transmission coefficients as a function frequency for square loop Array #1 of Table I at normal incidence.

This figure indicates that the equivalent circuit model can accurately predict the reflection and the transmission bands.

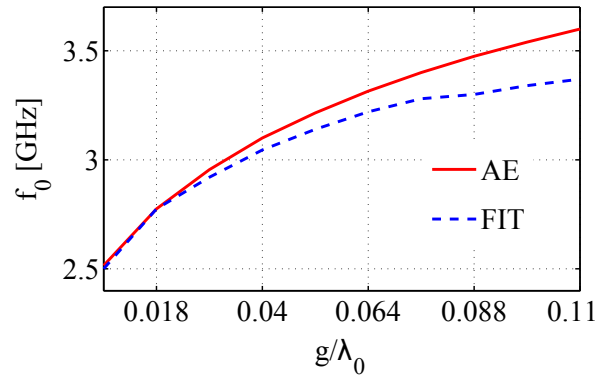


Fig. 3. Resonant frequency of transmission coefficient as a function of gap  $g$  variation for square loop Array #2 of Table I using the Analytical Equations (AE) compared to Finite Integration Technique Analysis (FIT) at normal incidence.

#### A. Effect of the Gap Width $g$

To investigate the model accuracy for different gap width  $g$ , the parameters of Array #2 (see Table I) are used to calculate the resonance frequency ( $f_0$ ) and compared to the one obtained by the FIT. The results shown in Fig. 3 are plotted as a function of gap variation ( $g/\lambda_0$ ). Here ( $\lambda_0$ ) is calculated from the resonance frequency ( $f_0$ ) calculated by FIT. It can be noticed that the equivalent circuit model diverges from the results obtained by FIT as the gap increases. This limitation is directly due to the assumption of treating the neighboring vertical conductors as one conductor which is twice the width of the single side (Eq. 2). However, this is only possible when the gap is reasonably small.

#### B. Effect of the Dielectric Substrate Material

The effect of dielectric substrate bonding the array elements was investigated in [11]. For thin dielectric layers the value of the capacitance varies as a function of dielectric thickness  $t$ . A value of the effective permittivity is calculated throughout an iterative procedure for thin dielectric substrates in [12]. The expression depends on both  $\epsilon_r$  and  $t$  and the resulting effective permittivity can be included in the equivalent circuit model by multiplying the subsceptance  $B_C$ . The expression of the effective permittivity ( $\epsilon_{eff}$ ) is obtained as:

$$\epsilon_{eff} = \epsilon_r + (\epsilon_r - 1) \cdot \left[ \frac{-1}{e^{x \cdot N}} \right] \quad (10)$$

where

$$x = 10 \cdot t/p \quad (11)$$

$t$  is the thickness of the substrate,  $p$  is the periodicity and  $N$  is an exponential factor that vary with the geometry of the unit cell. For square-loop arrays,  $N$  is around 1.8. When the width  $W$  is large compared with the global dimensions of the unit cell,  $N$  decreases accordingly (i.e. for metal patches  $N=1.3$ )

For the square-loop FSS the value of the susceptance is, therefore, modified as:

$$B_C = 4 \cdot \epsilon_{eff} \cdot \frac{1}{Z_0} \left( \frac{d}{p} \right) F(p, g, \lambda) \quad (12)$$

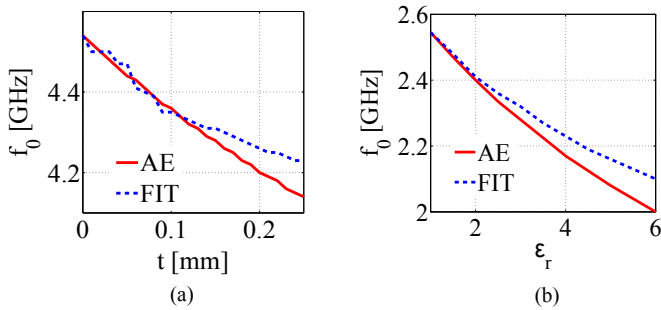


Fig. 4. Resonance Frequency as a function of substrate thickness variation  $t$  variation for square loop Array #3 of Table I using the analytical equations (AE) compared to finite integration technique (FIT) at normal incidence.

To investigate the effect of the dielectric substrate, the resonant frequency is calculated by the equivalent circuit model and by the FIT, and the results are plotted as a function of thickness variation in Fig. 4-a and as a function of substrate permittivity in Fig. 4-b. It can be concluded from the figures that the equivalent circuit model approximates the results obtained by full wave analysis up to a very thin substrate (about 0.1 mm for Array #3). For the permittivity investigation, the parameters of Array #4 (Table I) are used to calculate the resonance frequency. It is also shown that the presented model holds for a low substrate permittivity ( $\epsilon_r < 3$ ). In the following section, the gridded-square-loop FSS is investigated.

### III. GRIDDED-SQUARE-LOOP ARRAYS

The Gridded-Square-Loop (GSL) configuration and its equivalent circuit model are shown in Fig. 5-a and Fig. 5-b respectively.  $p$  is the periodicity,  $d$  is the square side length,  $g$  is the gap between the inductive grid and the square loops,  $W_1$  is the width of the grid and  $W_2$  is the width of the squares. The presence of the grid is represented by an inductor inserted in parallel to the LC resonant circuit. The analytical equations are derived as follow:

$$Z_{fss} = \frac{Z_g \cdot Z_s}{Z_g + Z_s}. \quad (13)$$

where  $Z_g$  represents the grid impedance given by:

$$Z_g = jX_2 \quad (14)$$

and  $Z_s$  the square impedance derived as:

$$Z_s = j(X_1 - 1/B_1) \quad (15)$$

The values of  $X_1$ ,  $X_2$  and  $B_1$ :

$$X_1 = \omega L_1 = Z_0 \cdot 2 \cdot \frac{X_2 * X_3}{X_2 + X_3}, \quad (16)$$

$$X_2 = \omega L_2 = Z_0 \cdot F(p, w_1, \lambda), \quad (17)$$

$$X_3 = Z_0 \left( \frac{d}{p} \right) F(p, 2w_2, \lambda), \quad (18)$$

$$B_1 = \omega C_1 = \frac{2}{Z_0} \cdot \epsilon_{eff} \left( \frac{d}{p} \right) F(p, g, \lambda). \quad (19)$$

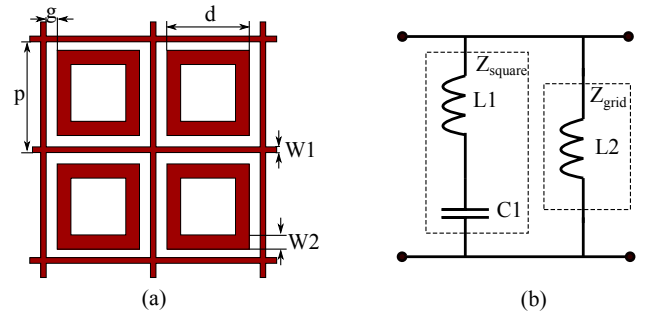


Fig. 5. Gridded Square Loop configuration and its equivalent circuit model

### A. Model Verification Using Full Wave Analysis

The reflection and the transmission coefficients vs. frequency for a GSL unit-cell with  $d = 12\text{ mm}$ ,  $g = 1.5\text{ mm}$ ,  $W_1 = 3\text{ mm}$  and  $W_2 = 1\text{ mm}$  are calculated and compared with the simulation results obtained using CST microwave studio. Fig. 6 shows the amplitude of the transmission and the reflection coefficients of the simulated unit cell as a function of frequency for a TE incident wave at an incident angle of  $\theta = 45^\circ$ . The figure shows that the equivalent circuit model can accurately predict the reflection and the transmission bands.

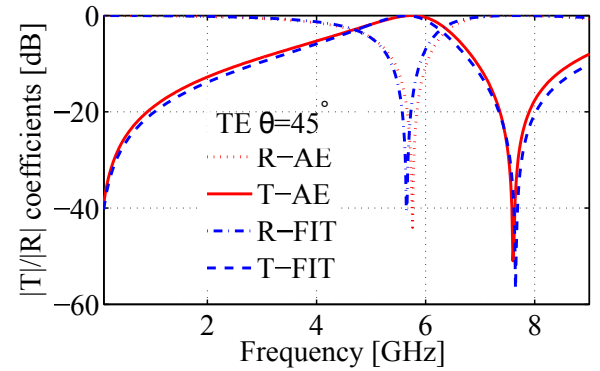


Fig. 6. Amplitude of the transmission and reflection coefficients vs. frequency at  $\theta = 45^\circ$  incidence, using Analytical Equations (AE) and Finite Integration Technique (FIT).  $d = 12\text{mm}$ ,  $g = 1.5\text{mm}$ ,  $W_1 = 3\text{mm}$  and  $W_2 = 1\text{mm}$

Since the equivalent circuit model is accurate enough to be used as a starting point in the initial design phase. The equivalent circuit model is extended to include any combination of a lumped-element circuit in the next section.

### IV. TUNABLE GRIDDED-SQUARE-LOOP FSS

The next step in the design, consists of loading lumped elements in the metal grid of the gridded square loop structure. Lumped elements can be added to the equivalent circuit model, therefore the behavior of the transmission characteristics can be predicted and controlled. Fig. 7 shows the loaded gridded-square-loop configuration and its equivalent circuit model. It is indicated in the figure that the unit cell is loaded with two lumped elements for each polarisation. This is necessary

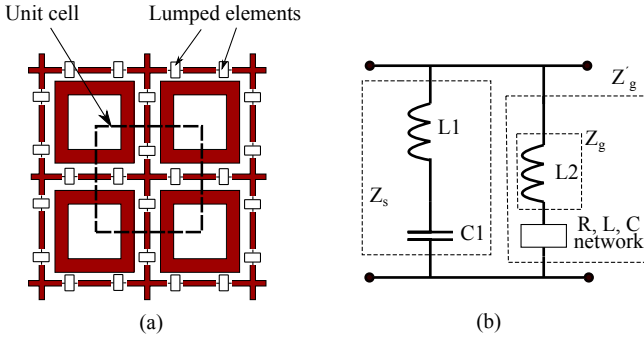


Fig. 7. Gridded square loop configuration loaded with lumped elements and the suggested equivalent circuit model

in order to be coherent with image theory (lumped elements cannot be placed on the symmetry planes nor on the periodic boundaries).  $Z_g'$  is the partial impedance of the grid and  $Z_s$  is the impedance given by the inner square loops. 2 lumped elements are added to the grid for both polarizations (TE and TM) which returns a total of 4 elements per unit cell, each of them, having an equivalent impedance  $Z_{eq}$ .

#### A. FSS loaded with a Parallel RC Combination

In this subsection, the frequency response due to the parallel combination of a capacitor and a resistor inserted in the grid is investigated. The grid impedance  $Z_g'$  is given by:

$$Z_g' = n \cdot \left[ R_a - j \left( X_a - \frac{X_2}{n} \right) \right], \quad (20)$$

where:

$$R_a = \frac{R_{load}}{\left[ (B_{load} \cdot R_{load})^2 + 1 \right]}, \quad (21)$$

and:

$$X_a = R_a \cdot R_{load} \cdot B_{load}. \quad (22)$$

Applying the same procedures as before, the square impedance  $Z_s$  and the FSS impedance  $Z_{fss}$  are calculated using Eq. 15 and Eq. 13 respectively. The unit cell dimensions used for the calculation of the transmission and reflection

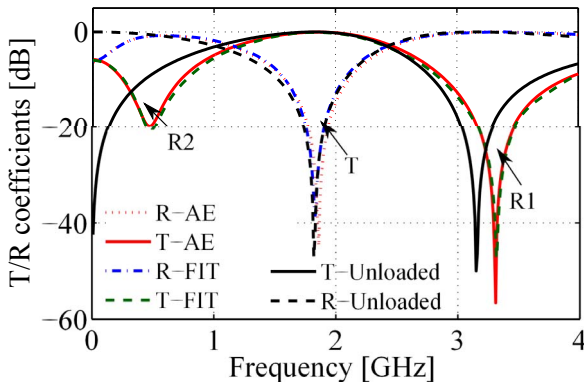


Fig. 8. Transmission and reflection coefficients of a unit cell of a GSL-FSS loaded with a capacitor ( $C_{load} = 10 \text{ pF}$ ) in parallel a resistor ( $R_{load} = 100\Omega$ ). Calculated using Analytical Equations (AE) and compared with FIT.

coefficients are:  $d = 31\text{mm}$ ,  $g = 2\text{mm}$ ,  $W1 = 1\text{mm}$  and  $W2 = 4.5\text{mm}$ , backed on a dielectric substrate with  $\epsilon_r = 3$  and thickness  $t = 125\mu\text{m}$ .

Fig. 8 shows the transmission and the reflection coefficients as a function of frequency calculated by the analytical equations and by the FIT. It is shown in the figure that the analytical solution can accurately predict the transmission and the reflection bands of the FSS. It is again shown that a new reflection band R2 is created when the grid is loaded with the capacitor and the resistor.

#### V. CONCLUSION

In this paper an equivalent circuit model is presented to calculate the transmission and the reflection bands of different frequency selective surfaces including the square loop FSS and the gridded square loop FSS. It is shown that the model is only valid to characterize FSS backed on a thin and low permittivity substrates. The equivalent circuit model is then extended for the insertion of lumped elements in the grid. The derived equations are validated by full wave analysis simulations. The main advantage of the suggested lumped-elements FSS is that its frequency response can be tuned by only changing the load value without changing the FSS dimensions. One typical application is to use the gridded square loop FSS loaded with rectifiers to harvest RF power. The impedance of the rectifier is modeled as a resistor in series with a capacitor. Using the equivalent impedance of the rectifier one can predict the transmission and the reflection bands which are consequently the RF harvesting bands.

#### REFERENCES

- [1] F. Costa and A. Monorchio, "A frequency selective radome with wideband absorbing properties," vol. 60, no. 6, pp. 2740–2747, 2012.
- [2] R. Dubrovka, J. Vazquez, C. Parini, and D. Moore, "Multi-frequency and multi-layer frequency selective surface analysis using modal decomposition equivalent circuit method," *IET Microwaves, Antennas & Propagation*, vol. 3, no. 3, pp. 492–500, 2009.
- [3] C.-H. Tsao and R. Mittra, "A spectral-iteration approach for analyzing scattering from frequency selective surfaces," vol. 30, no. 2, pp. 303–308, 1982.
- [4] N. Marcuvitz, *Waveguide Handbook*. New York : McGraw-Hill, 1951.
- [5] A. E. Yilmaz and M. Kuzuoglu, "Design of the square loop frequency selective surfaces with particle swarm optimization via the equivalent circuit model," *Radioengineering*, vol. 18, pp. 95–102, 2009.
- [6] E. Fuad Kent, B. Dken, and M. Kartal, "A new equivalent circuit based fss design method by using genetic algorithm," in *2nd International Conference on Engineering Optimization*, September 6 - 9, 2010, Lisbon, Portugal.
- [7] R. J. Langley and E. A. Parker, "Equivalent circuit model for arrays of square loops," *Electronics Letters*, vol. 18, no. 7, pp. 294–296, 1982.
- [8] C. K. Lee and R. J. Langley, "Equivalent-circuit models for frequency-selective surfaces at oblique angles of incidence," *IEE Proceedings H Microwaves, Antennas and Propagation*, vol. 132, no. 6, pp. 395–399, 1985.
- [9] E. Parker, "The gentleman's guide to frequency selective surfaces," April 1991.
- [10] M. C. T. Weiland, "Discrete electromagnetism with the finite integration technique," *Progress In Electromagnetics Research*, vol. 32, pp. 65–87, 2001.
- [11] R. Luebbers and B. Munk, "Some effects of dielectric loading on periodic slot arrays," vol. 26, no. 4, pp. 536–542, 1978.
- [12] F. Costa, A. Monorchio, and G. Manara, "An equivalent circuit model of frequency selective surfaces embedded within dielectric layers," in *Proc. IEEE Antennas and Propagation Society Int. Symp. APSURSI '09*, 2009, pp. 1–4.